Electronic Supplementary Material (ESI) for CrystEngComm.

An Iron(II) Coordination Polymer of a Triazolyl *Tris*-Heterocycle Showing a Spin State Conversion Triggered by Loss of Lattice Solvent

Iurii Galadzhun, Izar Capel Berdiell, Namrah Shahid and Malcolm A. Halcrow*

School of Chemistry, University of Leeds, Woodhouse Lane, Leeds LS2 9JT, United Kingdom.
E-mail: m.a.halcrow@leeds.ac.uk

Supporting Information

Experimental

Synthesis of 2-fluoro-6-(pyrazol-1-yl)pyridine. This was synthesised by an alternative to the literature procedure.[1] Pyrazole (1.4 g, 20 mmol) was dissolved in a dmf (20 cm^3):thf (6 cm^3) solvent mixture, after which NaH (60 % dispersion in mineral oil; 0.8 g, 20 mmol) was slowly added. The mixture was stirred at room temperature for 10 mins until hydrogen evolution ceased, then 2,6-difluoropyridine (2.42 g, 21 mmol) was added. The reaction mixture was stirred for 20 h at room temperature, then quenched with water (250 cm^3). The mixture was extracted with Et_2O (5x 50 cm^3), and the combined organic layers were washed with water and brine, dried with $MgSO_4$ then evaporated to dryness. The oily residue was purified by flash silica column chromatography (99:1 dichloromethane:methanol eluent, rf 0.7), to yield the target product as a pale yellow oil which slowly deposited colourless crystals on standing. Yield 1.1 g, 34 %. Mp *ca* 20 °C. HR-ESI MS *m*/*z* 164.0610 (calcd for $[(C_8H_6FN_3)H]^+$ 164.0619), 186.0429 (calcd for $[(C_8H_6FN_3)Na]^+$ 186.0438). ^{1}H NMR ($CDCl_3$) δ 6.45 (dd, 1H, Pz *H*^{4}), 6.79 (dd, 1H, Py *H*^{5}), 7.72 (d, 1H, Pz *H*^{3}), 7.84 (m, 1H, Py *H*^{3}), 7.87 (pseudo-t, 1H, Py *H*^{4}), 8.46 (d, 1H, Pz *H*^{5}). ^{13}C NMR ($CDCl_3$) δ 106.1 (d, Py *C*^{3}), 108.3 (s, Pz *C*^{4}), 109.0 (d, Py *C*^{5}), 127.6 (s, Pz *C*^{5}), 142.8 (s, Pz *C*^{3}), 143.4 (d, Py *C*^{4}), 150.1 (d, Py *C*^{6}), 162.4 (d, Py *C*^{2}). ^{19}F NMR ($CDCl_3$) δ –68.3.

Synthesis of 2-(1,2,4-triazol-1-yl)-6-(pyrazol-1-yl)pyridine (*L*). This was synthesised by a different route from the literature report.[2] Solid NaH (60 % dispersion in mineral oil; 0.39 g, 9.8 mmol) was suspended in a dmf (3 cm^3)/thf (6 cm^3) solvent mixture. Solid 1,2,4-triazole (0.64 g, 9.2 mmol) was slowly added, and the mixture was then stirred at room temperature for 30 minutes. Solid 2-fluoro-6-(pyrazol-1-yl)pyridine (1.0 g, 6.1 mmol) was then added. The reaction mixture was stirred at 80 °C for 3 days under a $CaCl_2$ drying tube. After cooling to room temperature, the reaction mixture was slowly mixed with excess water, and the resultant white powder was collected, dried and analysed without further purification. Yield 1.2 g, 95 %. Mp 163-164 °C (lit 167-169 °C).[2] Found C, 56.8; H, 3.85; N, 39.4 %. Calcd for $C_{10}H_8N_6$ C, 56.6; H, 3.80; N, 39.6 %. HR-ESI MS *m*/*z* 213.1019 (calc. for $[(C_{10}H_8N_6)H]^+$ 213.0883), 235.0852 (calc. for $[(C_{10}H_8N_6)Na]^+$ 235.0703). ^{1}H NMR ($CDCl_3$) δ 6.52 (pseudo-t, 1H, Pz *H*^{4}), 7.77 (m, 2H, Pz *H*^{3} + Py *H*^{5}), 8.00 (m, 2H, Py *H*^{4} + *H*^{5}), 8.12 (s, 1H, Tz *H*^{3}), 8.55 (d, 1H, Pz *H*^{5}), 9.16 (s, 1H, Tz *H*^{5}). ^{13}C NMR ($CDCl_3$) δ 108.6 (Pz *C*^{4}), 110.1 and 111.5 (Py *C*^{3} + *C*^{5}), 127.2 (Pz *C*^{5}), 141.6 (Py *C*^{4}), 142.2 (Tz *C*^{5}), 142.9 (Pz *C*^{3}), 147.9 (Py *C*^{2}), 150.5 (Py *C*^{6}), 153.2 (Tz *C*^{3}).

Synthesis of $[Fe(\mu\text{-}L)_2\{Fe(L)_2(OH_2)_2\}][BF_4]_4$ (1). Filtered solutions of *L* (0.13 g, 0.58 mmol) and $Fe[BF_4]_2{\cdot}6H_2O$ (0.10 g, 0.29 mmol) in $MeNO_2$ (2x 5 cm^3) were mixed at room temperature, yielding an immediate yellow solution. Slow diffusion of di(*iso*propyl)ether vapour into the solution yielded the complex as clusters of orange prisms, which rapidly degrade to a yellow powder upon exposure to air. Yield 0.11 g, 56 %. Found C, 35.8; H, 2.63; N, 24.9 %. Calcd for $C_{40}H_{36}B_4F_{16}Fe_2N_{24}O_2$ C, 35.8; H, 2.70; N, 25.0 %.

Single Crystal Structure Analyses

Crystals of *L* were obtained from chloroform solution, while the crystallisation procedures for the other two compounds are described in their synthesis protocols above. Crystallographic data were measured with an Agilent Supernova dual-source diffractometer using monochromated Cu-K_α (λ = 1.5418 Å) radiation. The diffractometer was fitted with an Oxford Cryostream low-temperature device. Experimental details of the structure determinations in this study are given in Tables S1 and S2.

All the structures were solved by direct methods *(SHELXS97*[3]), and developed by full least-squares refinement on F^2 (*SHELXL97*[3]). Crystallographic figures were prepared using *XSEED*,[4] and octahedral coordination volumes (V_{Oh}) were calculated with *Olex2*.[5]

Structure refinement of 2-fluoro-6-(pyrazol-1-yl)pyridine. No disorder is present in the model, and no restraints were applied to the refinement. All non-H atoms were refined anisotropically, and H atoms were located in the Fourier map and refined positionally, with U_{iso} constrained to 1.2x U_{eq} of the corresponding C atom.

While this compound crystallises in a handed space group, the absolute structure of the crystal could not be unambiguously determined owing to its light atom composition. Hence the Friedel opposite reflections in those datasets were merged for their final least squares cycles.

Structure refinement of *L*. No disorder is present in the model, and no restraints were applied to the refinement. All non-H atoms were refined anisotropically, and H atoms were located in the Fourier map and refined positionally, with U_{iso} constrained to 1.2x U_{eq} of the corresponding C atom. A DFIX restraint was applied to one C–H bond to force it to refine to a reasonable value.

Structure refinement of 1·MeNO$_2$·*x*H$_2$O. The asymmetric unit contains half a repeating unit of the coordination polymer, with Fe(1) lying on a crystallographic C_2 axis and Fe(2) spanning an inversion centre. There are also two BF_4^- ions on general crystallographic sites; half a nitromethane molecule on a C_2 axis; and an additional lattice water site which was modelled as 0.67-occupied in the two lowest temperature structures, but whose occupancy evidently decreased to 0.50 at 250 K, and 0.33 at 290 K. The gradual loss of the lattice water during the higher temperature data collections is consistent with the observed facile loss of lattice solvent in the bulk material.

Two orientations of the 2-(pyrazolyl)pyridyl fragment of the unique bridging *L* ligand were resolved at each temperature. These ligand sites refined without restraints, but with temperature-dependent occupancy ratios ranging from 0.621(15):0.379(15) at 150 K to 0.513(6):0.487(6) at 290 K. The F atoms of both anions are also disordered over orientations, which were modelled with equal occupancies using refined B–F and F...F distance restraints. Lastly, the nitromethane half-molecule was disordered over two sites in the 250 and 290 K refinements, which shared a common N atom. These were treated with fixed C–N, N–O, O...O and C...O distance restraints.

All crystallographically ordered non-H atoms were refined anisotropically and C-bound H atoms were placed in calculated positions and refined using a riding model. The aqua ligand H atoms were located in the Fourier map and refined, with fixed O–H and H...H distance restraints and the constraint $U_{iso}\{H\} = 1.5x\ U_{eq}\{O\}$. The partial lattice water H atoms were not included in the model, but are accounted for in the molecular weight and density calculations.

CCDC-1950547-1950548 and 1951382-1951385 contain the supplementary crystallographic data for this paper (Table S1). These data can be obtained free of charge from The Cambridge Crystallographic Data Centre via **www.ccdc.cam.ac.uk/data_request/cif**.

Other measurements

Elemental microanalyses were performed by the microanalytical services at the London Metropolitan University School of Human Sciences. Electrospray mass spectra were recorded on a Bruker MicroTOF-q instrument, from chloroform solution. Sodium-containing species in the mass spectra originate from the sodium formate calibrant used. NMR spectra employed a Bruker DPX300 spectrometer operating at 300.1 MHz (^{1}H), 75.5 MHz (^{13}C) or 282 MHz (^{19}F).

Solid state magnetic susceptibility measurements were performed on a Quantum Design MPMS-3 magnetometer, with an applied field of 5000 G and a scan rate of 5 Kmin^{-1}. Freshly prepared **1**·MeNO$_2$·*x*H$_2$O was protected from solvent loss during the measurements with a drop of diethyl ether in the sealed sample holder, while the dried sample used for the other measurement had been stored *in vacuo* at room temperature for 18 hrs. A diamagnetic correction for the sample was estimated from Pascal's constants;[6] a diamagnetic correction for the sample holder was also applied.

Table S1 Experimental data for the organic ligand crystal structure determinations.

	2-Fluoro-6-(pyrazol-1-yl)pyridine	*L*
formula	$C_8H_6FN_3$	$C_{10}H_8N_6$
fw	163.16	212.22
crystal system	orthorhombic	monoclinic
space group	$P2_12_12_1$	$P2_1/c$
a / Å	4.0393(1)	12.5794(9)
b / Å	11.2187(4)	3.8549(3)
c / Å	16.2922(4)	20.4981(14)
α / °	–	–
β / °	–	103.627(7)
γ / °	–	–
V / Å^3	738.29(4)	966.02(12)
Z	4	4
T / K	120(2)	150(2)
μ (Cu-K_α) / mm^{-1}	0.943	0.804
D_{calcd} / gcm^{-3}	1.468	1.459
reflections measured	1711	4624
unique reflections	870	1947
R_{int}	0.013	0.033
parameters	127	169
restraints	0	0
R_1 [$I > 2\sigma(I)$][a]	0.028	0.052
wR_2 [all data][b]	0.079	0.135
GOF	1.079	1.135
$\Delta\rho_{min/max}$ / *e*Å^{-3}	–0.15/0.15	–0.18/0.30
Flack parameter	0.5(3)[c]	–
CCDC	1950547	1950548

[a] $R = \Sigma [|F_o| - |F_c|] / \Sigma |F_o|$ [b] $wR = [\Sigma w(F_o^2 - F_c^2)^2 / \Sigma w F_o^4]^{1/2}$

[c] The absolute structure of this light atom crystal was not determined.

Table S2 Experimental data for the crystal structures of $[Fe(\mu\text{-}L)_2\{Fe(OH_2)_2L_2\}][BF_4]_4\cdot MeNO_2\cdot xH_2O$ (**1**$\cdot MeNO_2\cdot xH_2O$) at different temperatures.

T / K	150 (x = 1.34)	200 (x = 1.34)	250 (x = 1)	290 (x = 0.66)
molecular formula	$C_{41}H_{41.68}B_4F_{16}Fe_2N_{25}O_{5.34}$	$C_{41}H_{41.68}B_4F_{16}Fe_2N_{25}O_{5.34}$	$C_{41}H_{41}B_4F_{16}Fe_2N_{25}O_5$	$C_{41}H_{40.32}B_4F_{16}Fe_2N_{25}O_{4.66}$
M_r	1429.05	1429.05	1422.93	1416.80
crystal class	monoclinic	monoclinic	monoclinic	monoclinic
space group	$C2/c$	$C2/c$	$C2/c$	$C2/c$
a / Å	19.9190(3)	19.9235(5)	19.9189(6)	19.9010(5)
b / Å	15.3887(3)	15.5984(5)	15.8603(5)	15.9683(4)
c / Å	18.5909(3)	18.6533(4)	18.7484(4)	18.7282(6)
α / °	–	–	–	–
β / °	101.152(2)	100.512(2)	99.528(2)	99.397(3)
γ / °	–	–	–	–
V / Å^3	5591.02(16)	5699.7(3)	5841.3(3)	5871.7(3)
Z	4	4	4	4
μ\{Cu-K_α\} / mm^{-1}	5.280	5.179	5.046	5.013
D_c / gcm^{-3}	1.698	1.665	1.618	1.603
measured reflections	19986	19798	11206	19128
independent reflections	5616	5714	5722	5822
R_{int}	0.033	0.041	0.052	0.045
parameters	447	447	452	453
restraints	63	63	75	75
R_1 [$F_0 > 4\sigma(F_0)$][a]	0.062	0.082	0.085	0.083
wR_2, all data[b]	0.161	0.231	0.250	0.245
goodness of fit	1.087	1.063	1.060	1.077
$\Delta\rho_{min/max}$ / eÅ^{-3}	–0.54/0.78	–0.73/0.89	–0.39/0.47	–0.53/0.51
CCDC	1951382	1951383	1951384	1951385

[a] $R = \Sigma[\,|F_o| - |F_c|\,] / \Sigma|F_o|$ [b] $wR = [\Sigma w(F_o^2 - F_c^2) \;/\; \Sigma wF_o^4]^{1/2}$

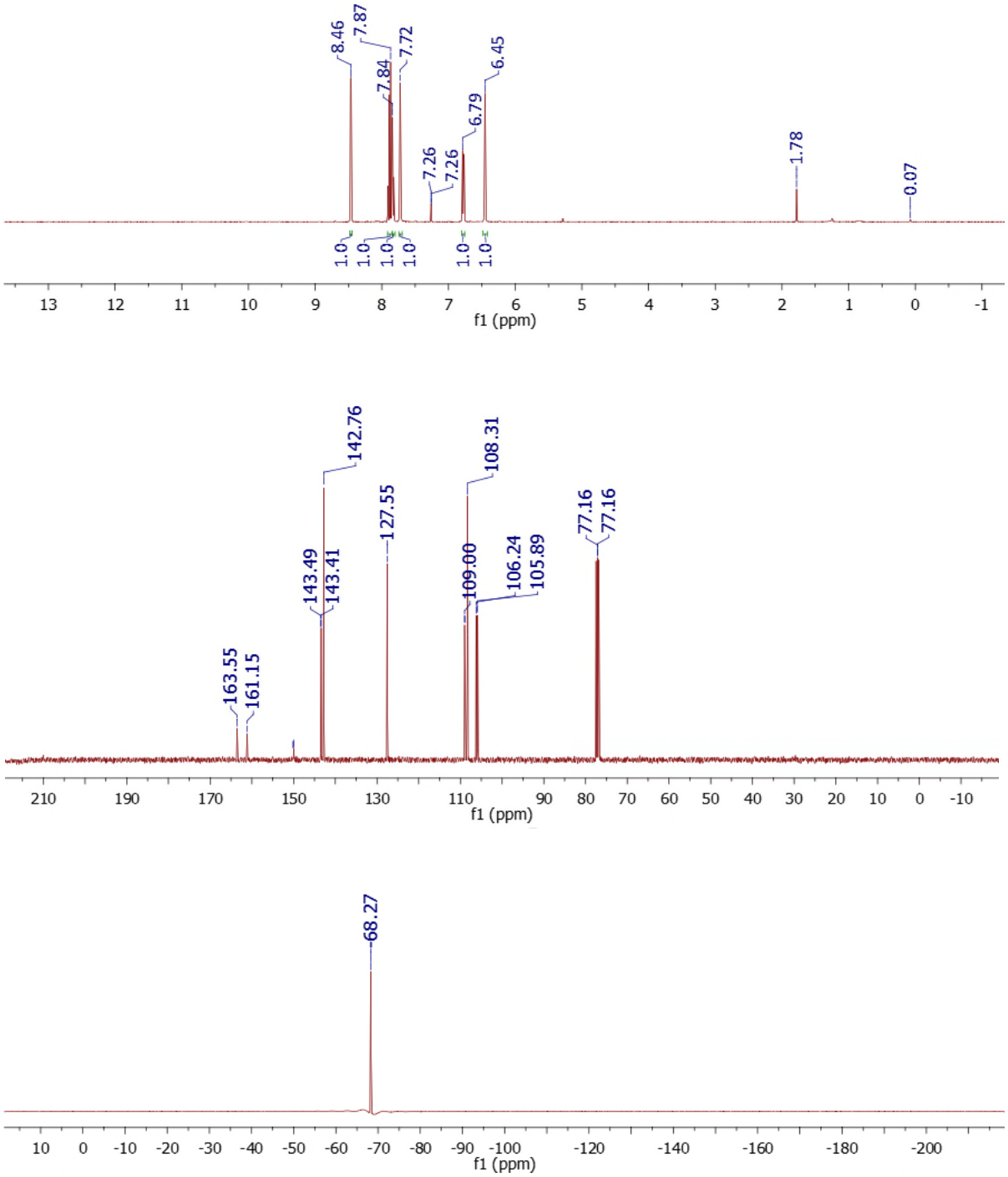

Figure S1 ^{1}H, ^{13}C and ^{19}F NMR spectra of 2-fluoro-6-(pyrazol-1-yl)pyridine ($CDCl_3$).

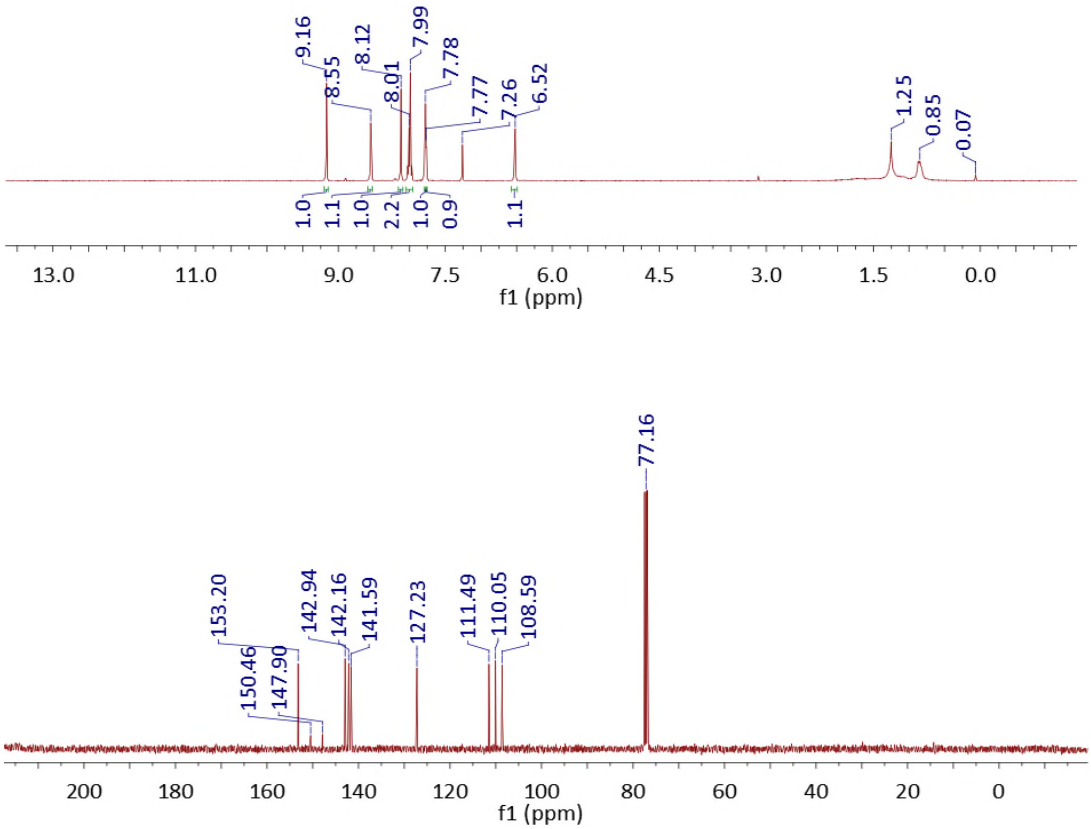

Figure S2 ^{1}H (top) and ^{13}C (bottom) NMR spectra of *L* ($CDCl_3$).

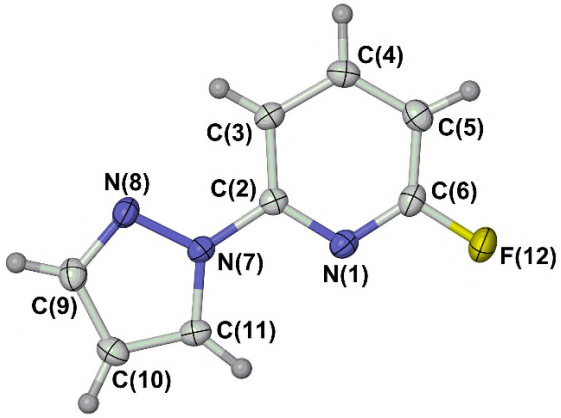

Figure S3 View of the molecule in the crystal structure of the ligand precursor compound 2-fluoro-6-(pyrazol-1-yl)pyridine. Displacement ellipsoids are at the 50 % probability level except for H atoms which have arbitrary radii.

Colour code: C, white; H, pale grey; F, yellow; N, blue.

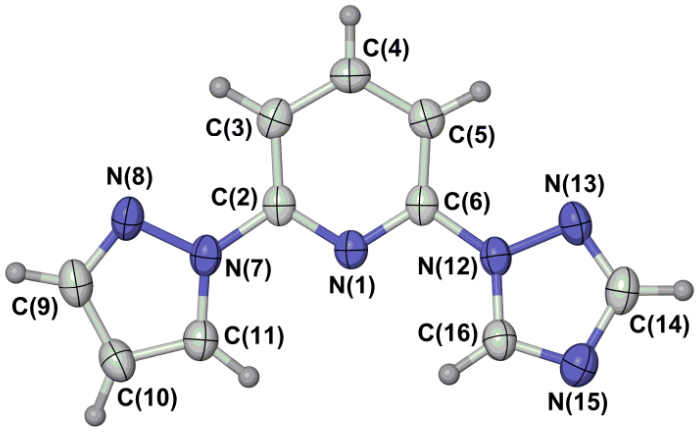

Figure S4 View of the molecule in the crystal structure of *L*. Displacement ellipsoids are at the 50 % probability level except for H atoms which have arbitrary radii.

Colour code: C, white; H, grey; N, blue.

While the pyridyl and pyrazolyl groups are essentially coplanar, as normal, the triazolyl ring is slightly twisted out of the plane of the other two heterocyclic groups. The dihedral angle between the least squares planes of the triazolyl and pyridyl rings is 10.50(13)°.

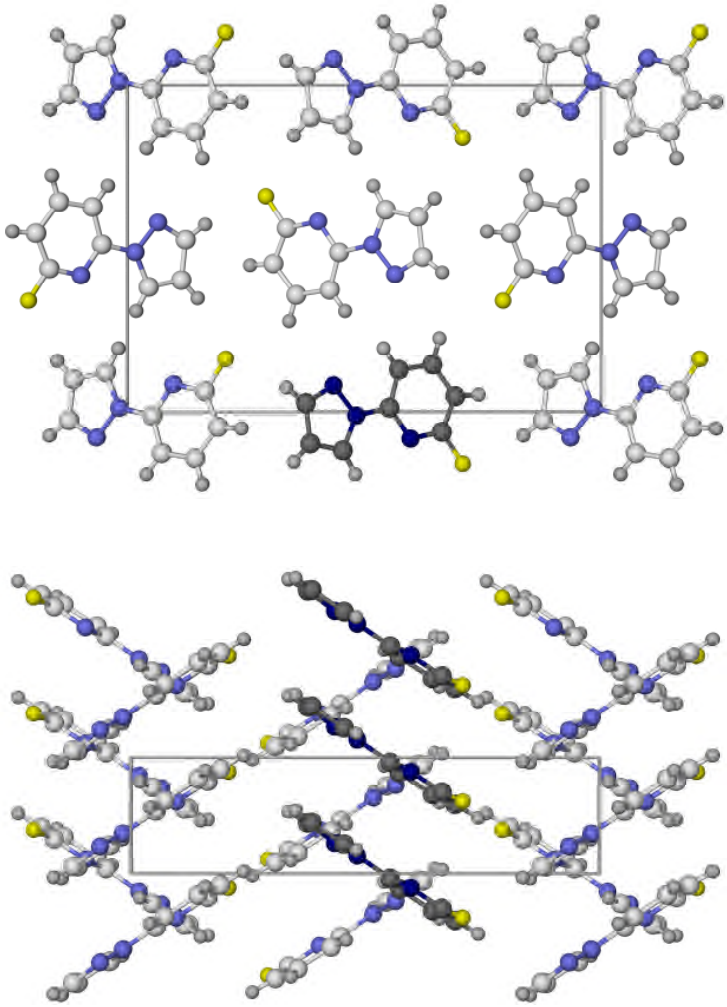

Figure S5 Packing diagram of 2-fluoro-6-(pyrazol-1-yl)pyridine. The views are: top, parallel to the (100) vector with *c* horizontal; and bottom, parallel to the (010) vector with *c* horizontal. One stack of molecules is highlighted with dark colouration.

Colour code: C, white or dark grey; H, grey; F, yellow; N, pale or dark blue.

The molecules associate into canted stacks by translation along *a*. The interplanar distance between nearest neighbour molecules in the stacks is 3.367(9) Å.

This structure is isomorphous with polymorph 3 of the related compound 2-fluoro-6-(indazol-2-yl)pyridine.[7]

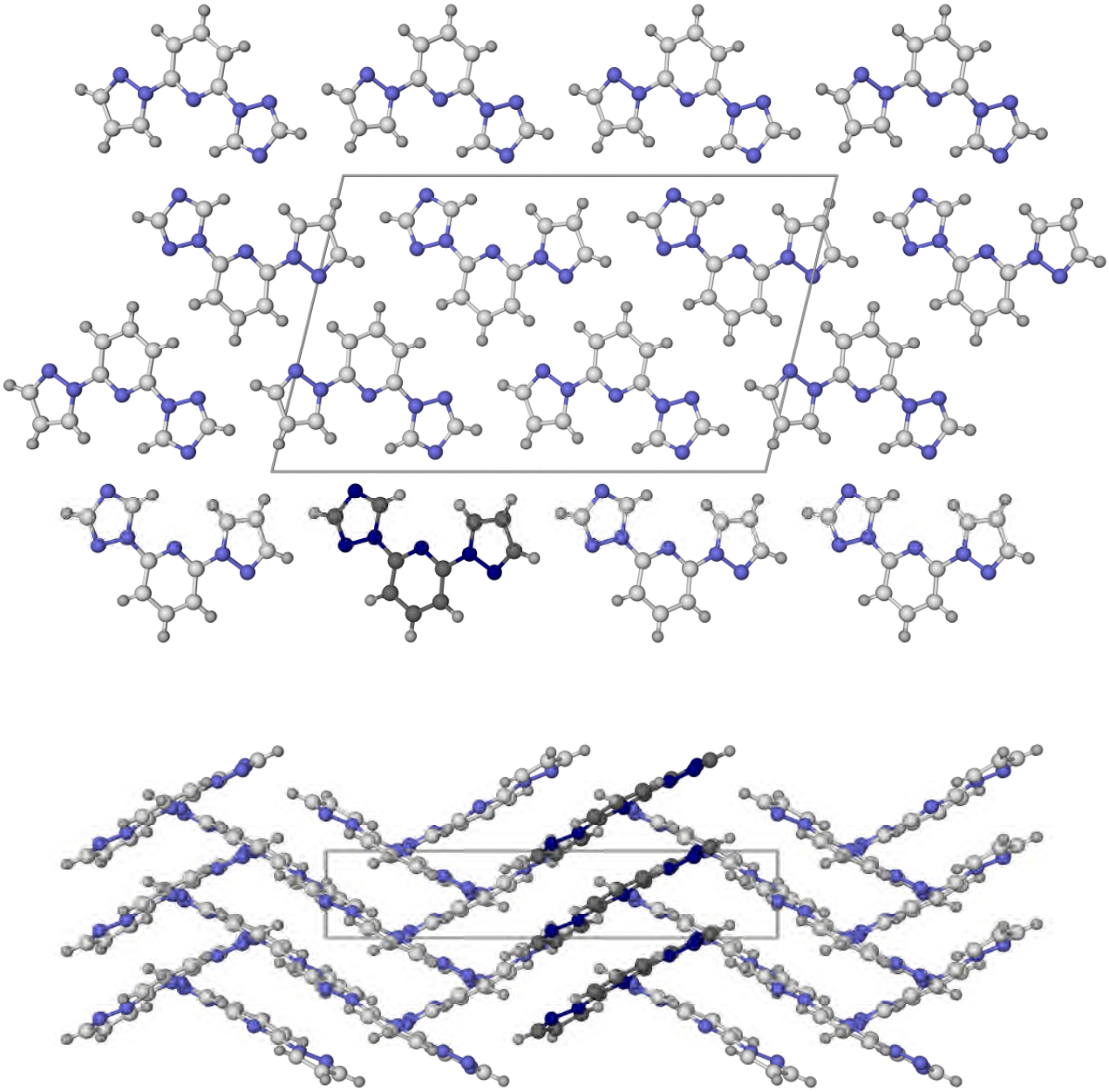

Figure S6 Packing diagram of *L*. The views are: top, parallel to the (100) vector with *c* horizontal; and bottom, parallel to the (001) vector with *a* horizontal. One stack of molecules is highlighted with dark colouration.

Colour code: C, white or dark grey; H, grey; N, pale or dark blue.

The molecules associate into canted stacks by translation along *b*. The interplanar distance between nearest neighbour molecules in the stacks is 3.330(3) Å.

Definitions of the structural parameters discussed in the paper

V_{Oh} is the volume (in Å^3) of the FeN_6 coordination octahedron in the complex molecule, which is typically <10 Å^3 in low-spin iron(II) compounds and ≥12 Å^3 in their high-spin form.[8]

Σ and Θ are defined as follows:

$$\Sigma = \sum_{i=1}^{12} |90 - \beta_i| \qquad \Theta = \sum_{j=1}^{24} |60 - \gamma_j|$$

where β_i are the twelve *cis*-N–Fe–N angles about the iron atom and γ_i are the 24 unique N–Fe–N angles measured on the projection of two triangular faces of the octahedron along their common pseudo-threefold axis (Scheme S1). Σ is a general measure of the deviation of a metal ion from an ideal octahedral geometry, while Θ more specifically indicates its distortion towards a trigonal prismatic structure. A perfectly octahedral complex gives $\Sigma = \Theta = 0$.

Σ and Θ were originally introduced to quantify small differences in the coordination geometries of high-spin iron(II) complexes of polydentate ligands.[9] More recently, they were popularized by Guionneau *et al.* as a way of confirming the spin state of a metal ion in a crystal structure; and to quantify the magnitude of the structural changes taking place during spin-crossover.[8]

Typical values for these parameters for compounds related to **1** are summarised in the footnote to Table S4.

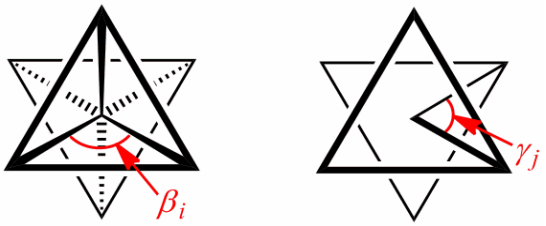

Scheme S1 Angles used in the definitions of the coordination distortion parameters Σ and Θ.[6]

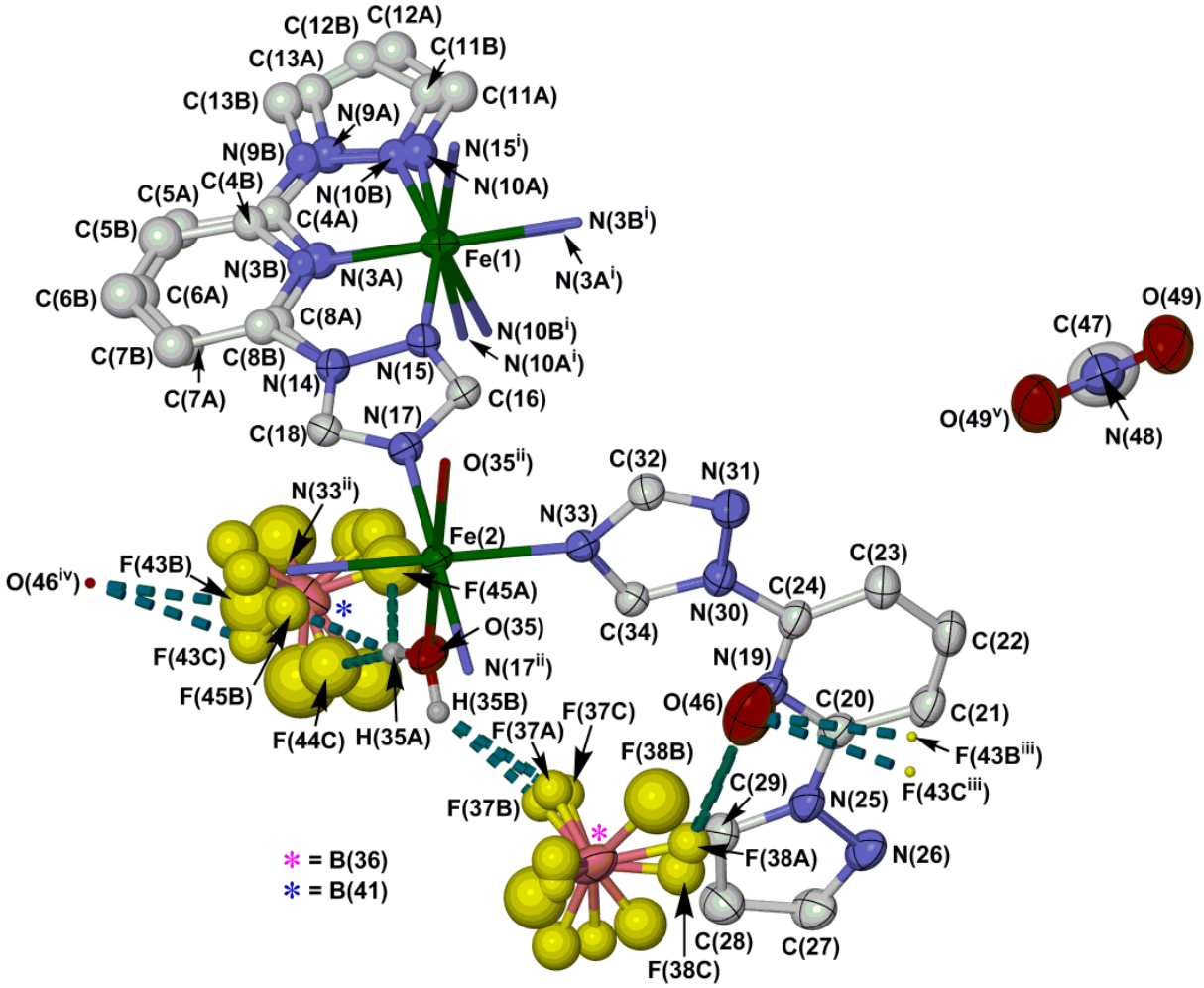

Figure S7 The asymmetric unit of **1**·$MeNO_2$·xH_2O at 150 K, showing the full atom numbering scheme (only F atoms participating in hydrogen bonding are labelled, for clarity). All non-H atoms are plotted with 50 % displacement ellipsoids, and C-bound H atoms are omitted. Symmetry codes: (i) 1–*x*, *y*, ½–*z*; (ii) 1–*x*, –*y*, 1–*z*; (iii) –½+*x*, –½+*y*, *z*; (iv) ½+*x*, ½+*y*, *z*; (v) –*x*, *y*, ½–*z*.

Colour code: C, white; H, pale grey; B, pink; F, yellow; Fe, green; N, blue; O, red.

The distance O(46)...F(38B) is 2.151(12) Å, which is *ca* 0.5 Å too short for an O–H...F hydrogen bond. We conclude that O(46) and the 'B' disorder site of anion B(36)-F(40) can't co-exist in a particular asymmetric unit, and thus that the disorder of that anion is coupled to the presence or absence of O(46) at each lattice site.

While there is no comparable steric clash between O(46) and anion B(41^{iii})-F(45^{iii}), the 'A' disorder site of that anion has no F atom within hydrogen bonding distance of O(46). Hence, the occupancy of O(46) might also influence the disorder in that anion, whose 'A' disorder orientation would be favoured when O(46) is absent.

Other intermolecular contacts that may influence the disorder in the structure are shown in Figure S9.

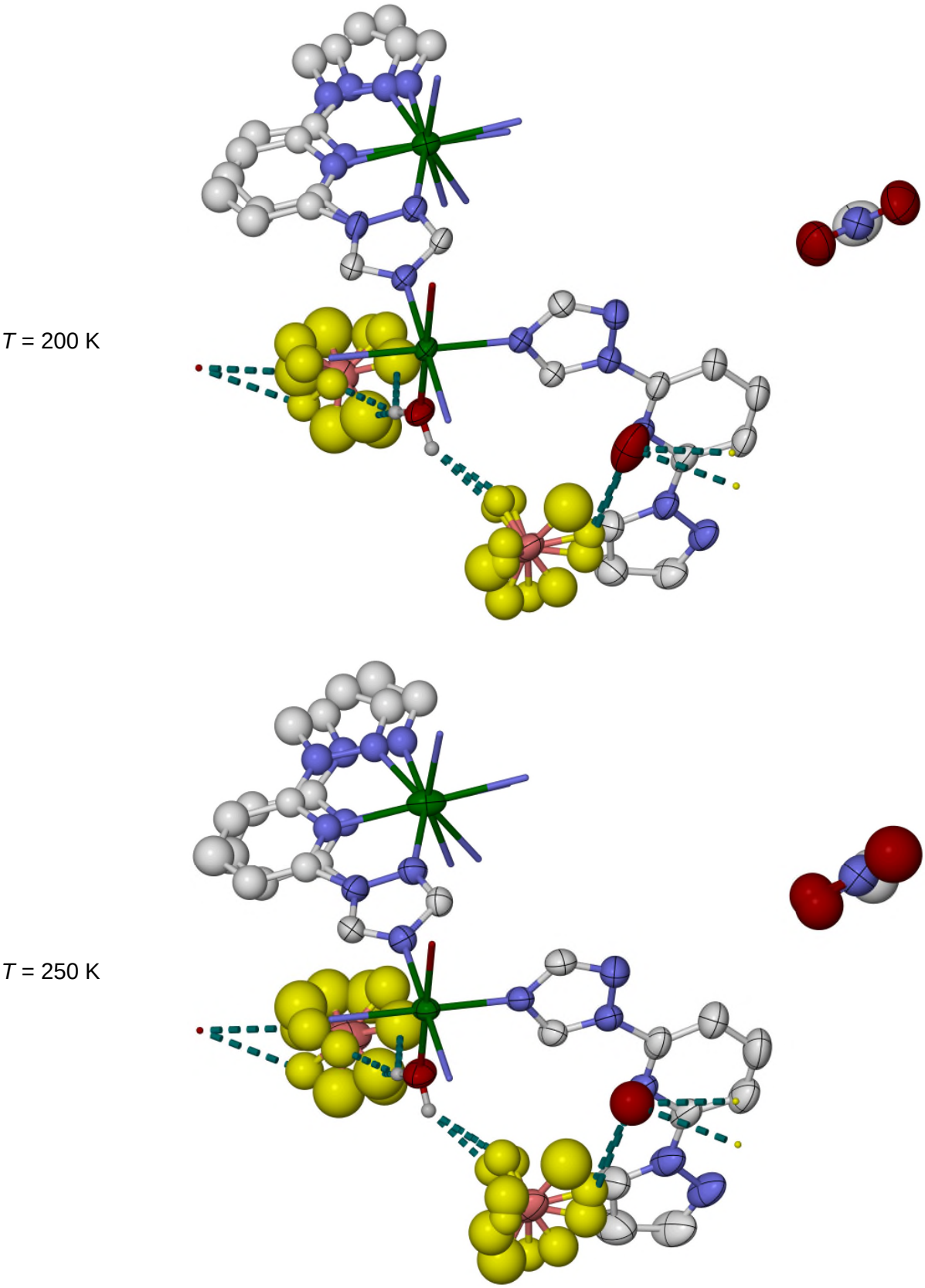

Figure S8 The asymmetric unit of **1**·$MeNO_2$·xH_2O at higher temperatures, in the same view as in Figure S7. Symmetry-generated disorder sites of the nitromethane half-molecule at 250 and 290 K are not included for clarity. Other details as for Figure S7.

T = 290 K

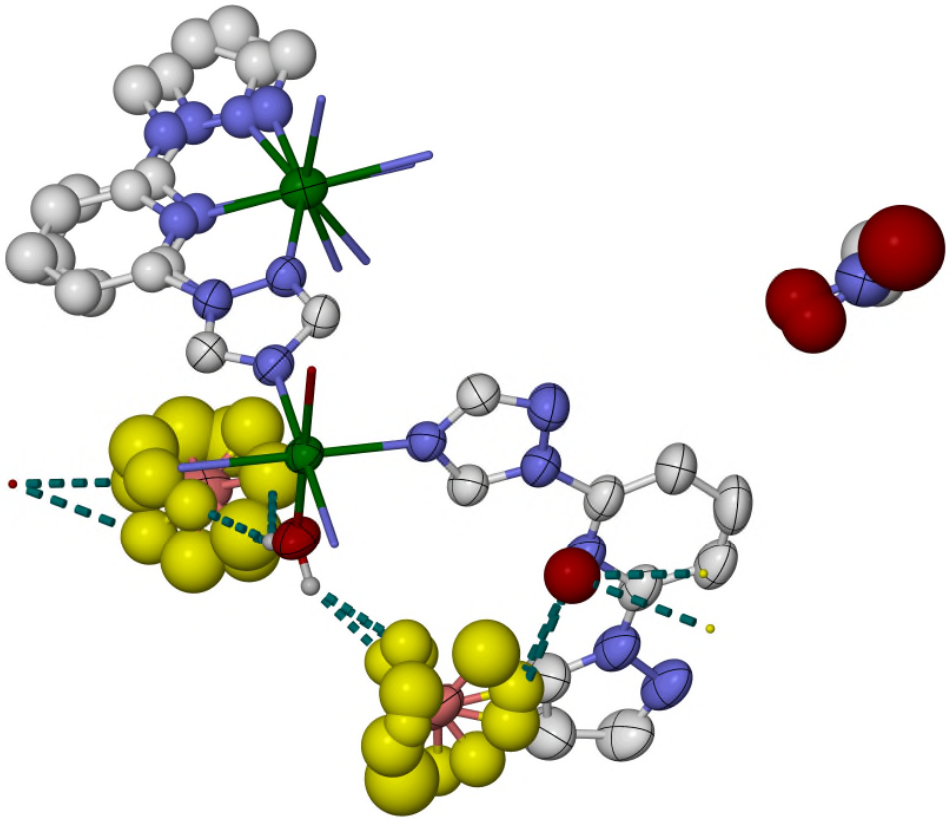

Figure S8 continued.

The occupancy of the partial lattice water molecule O(46) (Figure S7) in these refinements is: 0.67 at 150 and 200 K; 0.50 at 250 K; and 0.33 at 290 K. The total occupancy of the nitromethane half-molecule is 0.5 at each temperature.

p

Table S3 Selected bond lengths (Å) and angles (°) for **1**·$MeNO_2$·xH_2O. See Figure S7 for the atom numbering scheme. Symmetry codes: (i) 1–*x*, *y*, ½–*z*; (ii) 1–*x*, –*y*, 1–*z*.

T / K	150	200	250	290
Fe(1)–N(3A)/N(3B)	1.806(7)/2.045(11)	1.872(7)/2.159(12)	1.913(9)/2.324(12)	1.940(9)/2.268(9)
Fe(1)–N(10A)/N(10B)	1.970(6)/2.015(9)	1.994(6)/2.114(11)	2.089(9)/2.255(12)	2.098(9)/2.207(9)
Fe(1)–N(15)	2.013(3)	2.082(3)	2.196(5)	2.208(3)
Fe(2)–N(17)	2.233(3)	2.230(3)	2.217(4)	2.214(3)
Fe(2)–N(33)	2.186(3)	2.192(3)	2.188(4)	2.192(3)
Fe(2)–O(35)	2.101(2)	2.103(3)	2.102(4)	2.107(3)
N(3A)–Fe(1)–N(3A^{i})/N(3B)–Fe(1)–N(3A^{i})/N(3B)–Fe(1)–N(3B^{i})[a]	170.2(4)/174.5(3)/179.1(6)	170.2(4)/173.2(3)/179.1(6)	167.8(6)/176.0(4)/175.6(6)	168.7(5)/175.0(3)/177.9(4)
N(3A)–Fe(1)–N(10A)/N(3B)–Fe(1)–N(10A)/N(3B)–Fe(1)–N(10B)[a]	82.6(3)/86.5(3)/76.3(4)	80.6(3)/88.1(4)/74.7(5)	79.8(4)/86.2(4)/69.8(5)	78.8(4)/84.7(4)/71.5(3)
N(3A)–Fe(1)–N(10A^{i})/N(3B)–Fe(1)–N(10A^{i})/N(3B)–Fe(1)–N(10B^{i})[a]	90.4(3)/92.9(3)/103.0(4)	92.4(3)/92.6(3)/106.0(4)	91.7(4)/96.9(4)/113.2(4)	93.4(4)/96.7(4)/110.0(3)
N(3A)–Fe(1)–N(15)/N(3B)–Fe(1)–N(15)	81.3(2)/77.4(3)	80.3(2)/72.8(3)	77.0(3)/70.3(3)	77.0(3)/70.8(2)
N(3A)–Fe(1)–N(15^{i})/N(3B)–Fe(1)–N(15^{i})	105.7(2)/103.3(3)	106.7(2)/106.5(3)	111.8(3)/106.4(3)	111.3(2)/107.7(2)
N(10A)–Fe(1)–N(10A^{i})/N(10B)–Fe(1)–N(10A^{i})/N(10B)–Fe(1)–N(10B^{i})[a]	89.9(4)/90.7(2)/93.2(5)	90.6(4)/91.8(3)/96.1(5)	91.8(5)/93.8(3)/100.2(6)	93.1(5)/94.1(2)/98.0(4)
N(10A)–Fe(1)–N(15)/N(10B)–Fe(1)–N(15)	163.8(2)/153.7(3)	160.8(2)/147.4(4)	156.5(3)/140.1(4)	155.3(3)/142.2(3)
N(10A)–Fe(1)–N(15^{i})/N(10B)–Fe(1)–N(15^{i})	91.22(19)/93.3(3)	91.7(2)/94.8(3)	92.8(3)/97.0(3)	92.8(3)/97.1(2)
N(15)–Fe(1)–N(15^{i})	92.14(15)	92.32(17)	92.2(2)	91.74(18)
N(17)–Fe(2)–N(17^{ii})	180	180	180	180
N(17)–Fe(2)–N(33)	91.29(10)	91.20(11)	91.50(16)	91.67(12)
N(17)–Fe(2)–N(33^{ii})	88.71(10)	88.80(12)	88.50(16)	88.33(12)
N(17)–Fe(2)–O(35)	89.87(10)	89.97(12)	90.17(17)	90.09(13)
N(17)–Fe(2)–O(35^{ii})	90.13(10)	90.03(12)	89.83(17)	89.91(13)
N(33)–Fe(2)–N(33^{ii})	180	180	180	180
N(33)–Fe(2)–O(35)	88.90(10)	89.06(12)	89.64(17)	89.63(13)
N(33)–Fe(2)–O(35^{ii})	91.10(10)	90.94(12)	90.36(17)	90.36(13)
O(35)–Fe(2)–O(35^{ii})	180	180	180	180

[a]Three values are listed, corresponding to Fe(1) coordinated by two ligands of disorder orientation A; one orientation A ligand and one orientation B ligand; and, two ligands of disorder orientation B.

Table S4 Structural parameters calculated for **1**·$MeNO_2$·xH_2O at different temperatures, which are characteristic for the metal ion spin state (Å^3, °). The 'A' and 'B' orientations refer to the ligand disorder sites about Fe(1) (Figures S7 and S8). Definitions of V_{Oh}, Σ and Θ are given on page S11.

T / K	150	200	250	290
Orientation A:B refined occupancy	0.621(15):0.379(15)	0.599(5):0.401(5)	0.554(5):0.446(5)	0.513(6):0.487(6)
V_{Oh} {Fe(1)} orientation A–A/A–B/B–B[a]	9.27(2)/9.90(2)/10.49(3)	10.00(2)/10.83(2)/11.68(4)	11.03(3)/12.36(3)/13.53(4)	11.29(3)/12.28(3)/13.18(3)
Σ {Fe(1)} orientation A–A/A–B/B–B[a]	69.1(9)/85.2(9)/117.1(12)	82.7(9)/99.9(10)/148.0(13)	103.0(12)/127.8(12)/185.4(13)	108.2(12)/128.6(10)/174.7(9)
Θ {Fe(1)} orientation A–A/A–B/B–B[a]	229/301/374	274/371/468	340/459/583	356/451/550
V_{Oh} {Fe(1)} weighted average	9.74(5)	10.67(5)	12.20(7)	12.24(6)
Σ {Fe(1)} weighted average	84(2)	101(2)	132(2)	134(2)
Θ {Fe(1)} weighted average	284	352	448	450
V_{Oh} {Fe(2)}	13.661(10)	13.701(11)	13.596(16)	13.628(12)
Σ {Fe(2)}	10.1(3)	8.7(4)	8.1(6)	8.5(4)
Θ {Fe(2)}	28	27	24	23

[a]Three values are listed, corresponding to Fe(1) coordinated by two ligands of disorder orientation A; one orientation A ligand and one orientation B ligand; and, two ligands of disorder orientation B.

Other things being equal, typical V_{Oh}, Σ and Θ values for a homoleptic iron(II) complex of a sterically unhindered di(azolyl)pyridine *tris*-chelate are:[10,11]

Low spin: $9.4 \leq V_{Oh} \leq 9.8$ Å^3; $80 \leq \Sigma \leq 92°$; $270 \leq \Theta \leq 300°$.

High spin: $12.3 \leq V_{Oh} \leq 12.9$ Å^3; $148 \leq \Sigma \leq 155°$; $460 \leq \Theta \leq 490°$.

Some individual values of these parameters for Fe(1) are outside the expected ranges, indicating the challenges in interpreting its ligand disorder model. However the weighted average values are in line with expectation and are self-consistent, so these are probably the best description of the structure.

Fe(2) has a higher value of V_{Oh}, and much lower Σ and Θ, because its monodentate ligation allows it to adopt a near-regular octahedral geometry. In comparison Fe(1), which is constrained by the tridentate *L* ligand bite angle, has a less regular coordination geometry and correspondingly higher distortion parameters.[8]

Table S5 Hydrogen bond metric parameters for **1**·$MeNO_2$·xH_2O at different temperatures (Å, °). See Figure S7 for the atom numbering scheme. Symmetry code: (iii) $-½+x, -½+y, z$.

	D−H	H…A	D…A	D−H…A
T = 150 K				
O(35)–H(35A)…F(45A)/F(45B)/F(44C)	0.88(2)	2.30(4)/1.93(3)/1.78(2)	2.971(13)/2.742(8)/2.653(11)	133(4)/152(4)/171(4)
O(35)–H(35B)…F(37A)/F(37B)/F(37C)	0.88(2)	2.05(4)/2.02(4)/2.23(4)	2.733(8)/2.743(8)/2.881(8)	135(4)/139(5)/131(4)
O(46)...F(38A)/F(38C)[a]	–	–	2.654(11)/3.099(13)	–
O(46)...F(43B^{iii})/F(43C^{iii})[a]	–	–	2.709(12)/2.780(9)	–
T = 200 K				
O(35)–H(35A)…F(45A)/F(45B)/F(44C)	0.88(2)	2.22(5)/1.88(3)/1.77(3)	2.870(17)/2.700(9)/2.628(17)	130(5)/154(5)/163(6)
O(35)–H(35B)…F(37A)/F(37B)/F(37C)	0.88(2)	1.94(4)/2.00(4)/2.16(4)	2.711(8)/2.780(9)/2.886(10)	146(5)/148(6)/140(5)
O(46)...F(38A)/F(38C)[a]	–	–	2.699(14)/3.179(17)	–
O(46)...F(43B^{iii})/F(43C^{iii})[a]	–	–	2.688(14)/2.835(11)	–
T = 250 K				
O(35)–H(35A)…F(45A)/F(45B)/F(44C)	0.88(2)	2.21(6)/1.82(3)/1.84(4)	2.88(2)/2.639(14)/2.675(19)	133(6)/156(6)/158(7)
O(35)–H(35B)…F(37A)/F(37B)/F(37C)	0.88(2)	1.99(5)/1.97(5)/2.26(6)	2.691(12)/2.725(13)/2.924(13)	136(6)/142(7)/132(6)
O(46)...F(38A)/F(38C)[a]	–	–	2.77(2)/3.35(2)	–
O(46)...F(43B^{iii})/F(43C^{iii})[a]	–	–	2.708(18)/2.888(19)	–
T = 290 K				
O(35)–H(35A)…F(45A)/F(45B)/F(44C)	0.89(2)	2.16(5)/1.90(4)/1.80(3)	2.845(18)/2.680(11)/2.658(18)	134(5)/146(6)/163(7)
O(35)–H(35B)…F(37A)/F(37B)/F(37C)	0.89(2)	1.98(5)/1.93(4)/2.21(5)	2.710(10)/2.721(11)/2.911(10)	138(6)/147(6)/136(6)
O(46)...F(38A)/F(38C)[a]	–	–	2.78(2)/3.38(2)	–
O(46)...F(43B^{iii})/F(43C^{iii})[a]	–	–	2.684(18)/2.93(2)	–

[a]H atoms on the partial lattice water site O(46) were not located in the Fourier map, or included in the refinement.

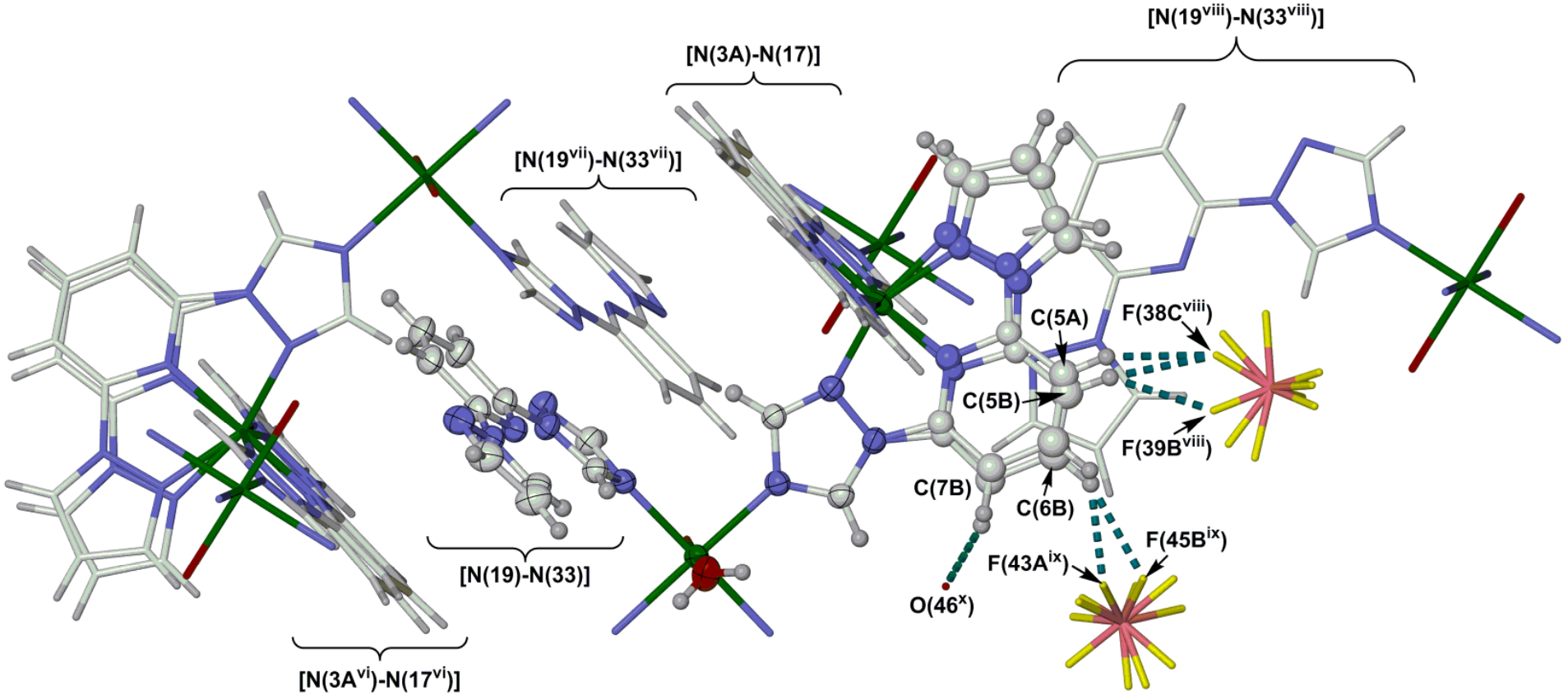

Figure S9 Other noteworthy intermolecular interactions in **1**·$MeNO_2$·xH_2O. All symmetry-generated residues are de-emphasised for clarity. Symmetry codes: (vi) $-^1/_2+x$, $^1/_2-y$, $^1/_2+z$; (vii) $^1/_2-x$, $^1/_2-y$, 1–z; (viii) $^1/_2+x$, $^1/_2-y$, $-^1/_2+z$; (ix) $^3/_2-x$, $^1/_2-y$, 1–z; (x) 1–x, –y, 1–z.

Colour code: C, white; H, pale grey; B, pink; F, yellow; Fe, green; N, blue; O, red.

The Figure shows the inter-chain $\pi...\pi$ interactions, and C–H...X contacts of <2.4 Å between disordered or partially occupied residues in the lattice. The latter imply the ligand disorder is connected to the anion disorder, and to the partial occupancy of O(46).

Metric parameters for these interactions at each temperature are listed in Table S6.

Table S6 Metric parameters for the intermolecular $\pi...\pi$ interactions, and C–H...X (X = O or F) contacts between disordered residues, in **1**·$MeNO_2$·xH_2O at different temperatures (Å, °). See Figures S7 and S9 for the atom numbering scheme. Symmetry codes: (vi) $-\frac{1}{2}+x, \frac{1}{2}-y, \frac{1}{2}+z$; (vii) $\frac{1}{2}-x, \frac{1}{2}-y, 1-z$; (viii) $\frac{1}{2}+x, \frac{1}{2}-y, -\frac{1}{2}+z$; (ix) $\frac{3}{2}-x, \frac{1}{2}-y, 1-z$; (x) $1-x, -y, 1-z$.

	H...X	Dihedral angle	Average interplanar distance	Horizontal offset
T = 150 K				
[N(19)-(29)]...[N(3A^{vi})-C(13A^{vi})]/[N(3B^{vi})-C(13B^{vi})]	–	6.9(2)/6.9(3)	3.29(3)/3.18(4)	2.12/2.05
[N(19)-C(34)]...[N(19^{vii})-C(34^{vii})]	–	0	3.316(10)	2.31
C(5A)–H(5A)...F(38C^{viii})	2.30	–	–	–
C(5B)–H(5B)...F(39B^{viii})/F(38C^{viii})	2.27/2.27	–	–	–
C(6B)–H(6B)...F(43A^{ci})/F(45B^{ci})/F(45C^{ci})	2.14/2.24/–[a]	–	–	–
C(7B)–H(7B)...O(46^{x})	2.15	–	–	–
T = 200 K				
[N(19)-(29)]...[N(3A^{vi})-C(13A^{vi})]/[N(3B^{vi})-C(13B^{vi})]	–	6.5(2)/7.8(3)	3.29(3)/3.25(4)	2.04/2.03
[N(19)-C(34)]...[N(19^{vii})-C(34^{vii})]	–	0	3.286(10)	2.38
C(5A)–H(5A)...F(38C^{viii})	2.23	–	–	–
C(5B)–H(5B)...F(39B^{viii})/F(38C^{viii})	2.29/2.33	–	–	–
C(6B)–H(6B)...F(43A^{ci})/F(45B^{ci})/F(45C^{ci})	1.85/2.16/2.14	–	–	–
C(7B)–H(7B)...O(46^{x})	2.12	–	–	–
T = 250 K				
[N(19)-(29)]...[N(3A^{vi})-C(13A^{vi})]/[N(3B^{vi})-C(13B^{vi})]	–	8.2(4)/6.4(4)	3.42(5)/3.19(6)	1.93/1.97
[N(19)-C(34)]...[N(19^{vii})-C(34^{vii})]	–	0	3.33(2)	2.33
C(5A)–H(5A)...F(38C^{viii})	2.23	–	–	–
C(5B)–H(5B)...F(39B^{viii})/F(38C^{viii})	2.11/2.33	–	–	–
C(6B)–H(6B)...F(43A^{ci})/F(45B^{ci})/F(45C^{ci})	1.84/2.25/2.11	–	–	–
C(7B)–H(7B)...O(46^{x})	1.96	–	–	–
T = 290 K				
[N(19)-(29)]...[N(3A^{vi})-C(13A^{vi})]/[N(3B^{vi})-C(13B^{vi})]	–	8.3(3)/5.8(3)	3.41(4)/3.25(4)	1.91/1.93
[N(19)-C(34)]...[N(19^{vii})-C(34^{vii})]	–	0	3.348(18)	2.35
C(5A)–H(5A)...F(38C^{viii})	2.26	–	–	–
C(5B)–H(5B)...F(39B^{viii})/F(38C^{viii})	2.17/2.32	–	–	–
C(6B)–H(6B)...F(43A^{ci})/F(45B^{ci})/F(45C^{ci})	1.93/2.27/2.24	–	–	–
C(7B)–H(7B)...O(46^{x})	2.02	–	–	–

[a]This value (2.46 Å) is too long to be considered a C–H...F contact at this temperature

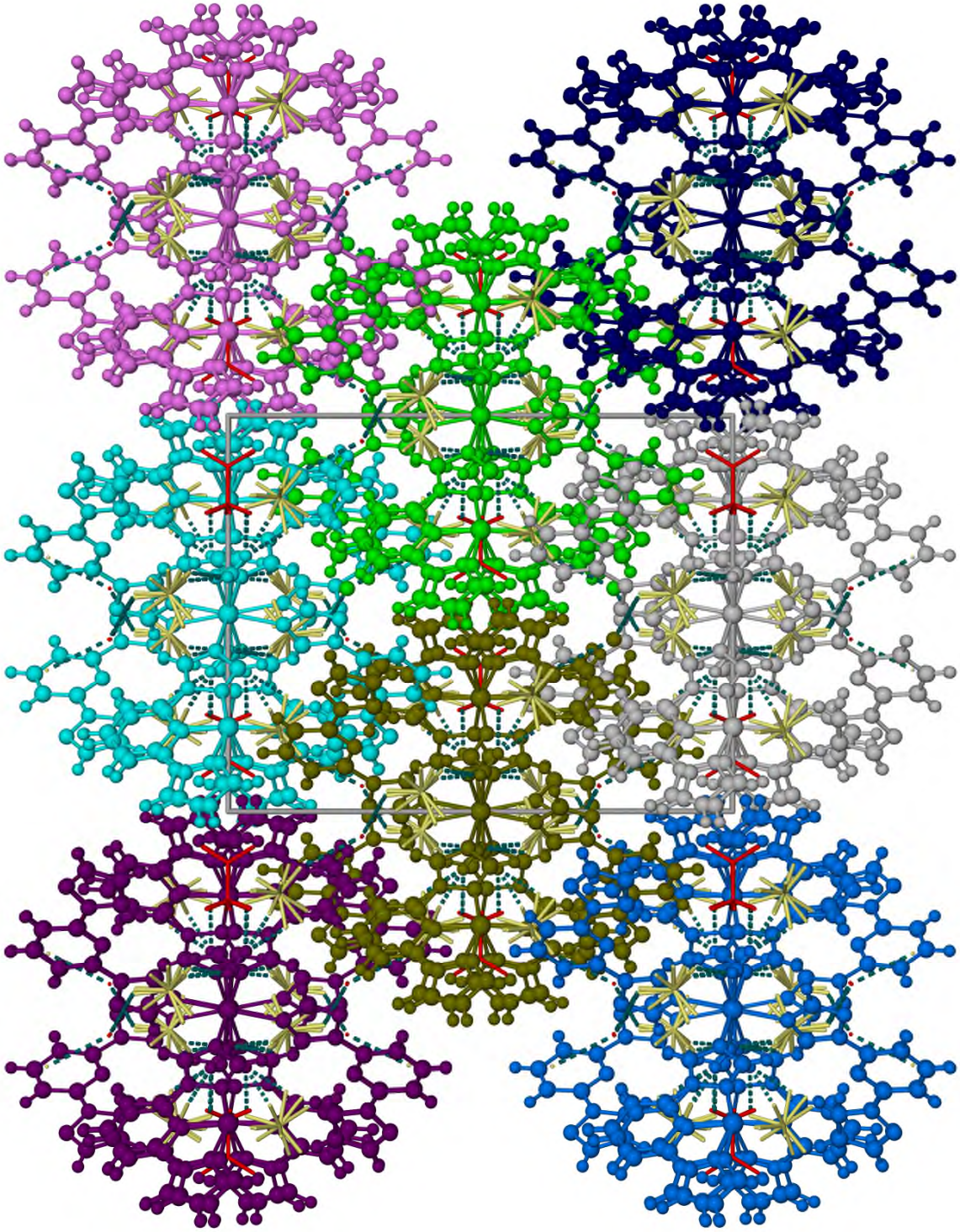

Figure S10 Packing diagram of **1**·$MeNO_2$·*x*H_2O at 150 K, viewed parallel to the coordination polymer chains. The orientation is parallel to the (001) vector with *a* horizontal. All orientations of the disordered residues are included.

Different coordination polymer chains are highlighted with different colouration, while the BF_4^- ions (yellow) and lattice solvent (red) are de-emphasised for clarity.

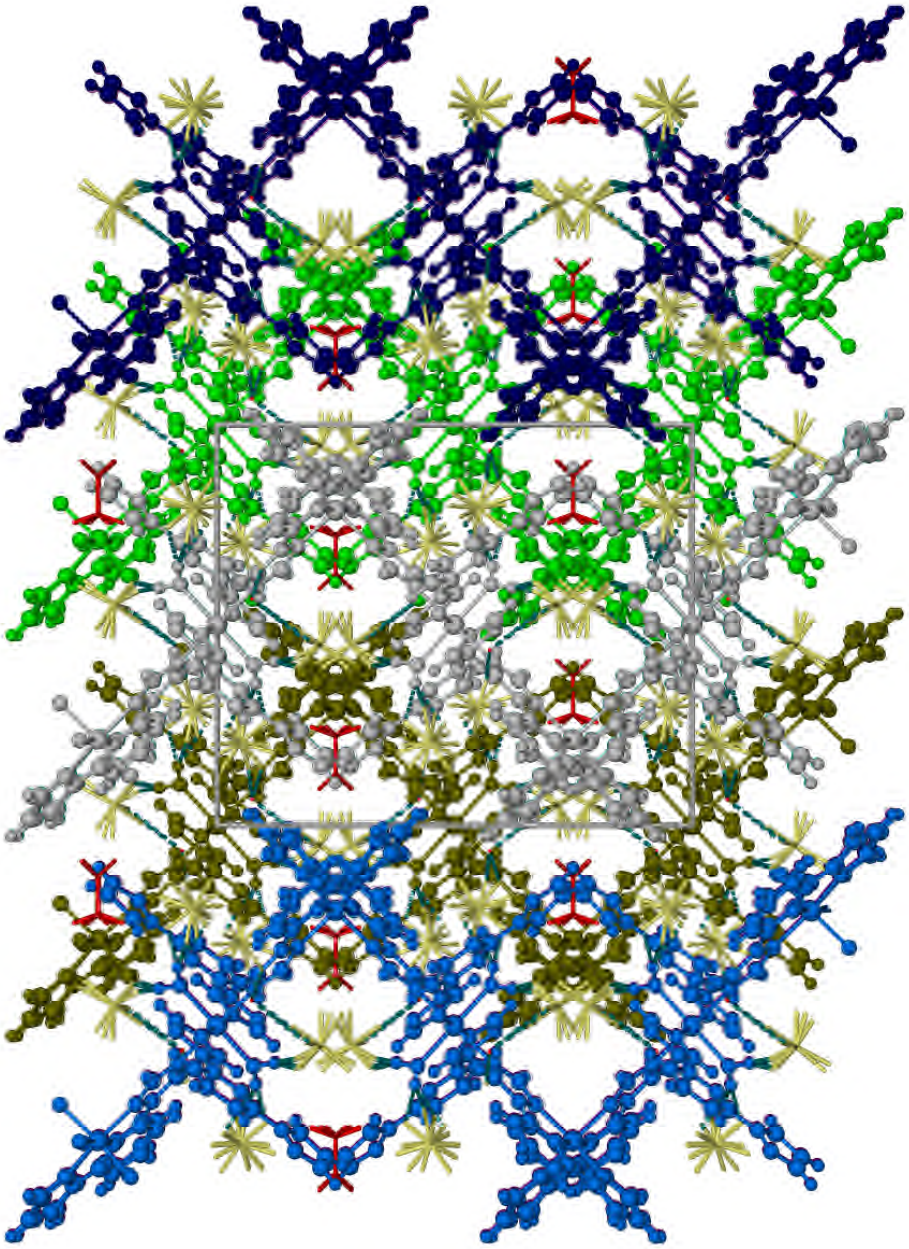

Figure S11 Alternative packing diagram of **1**·$MeNO_2$·xH_2O at 150 K, viewed perpendicular to the coordination polymer chains. The view is parallel to the (100) vector with *c* horizontal.

Other details as for Figure S10, including the colouration of the individual polymer chains.

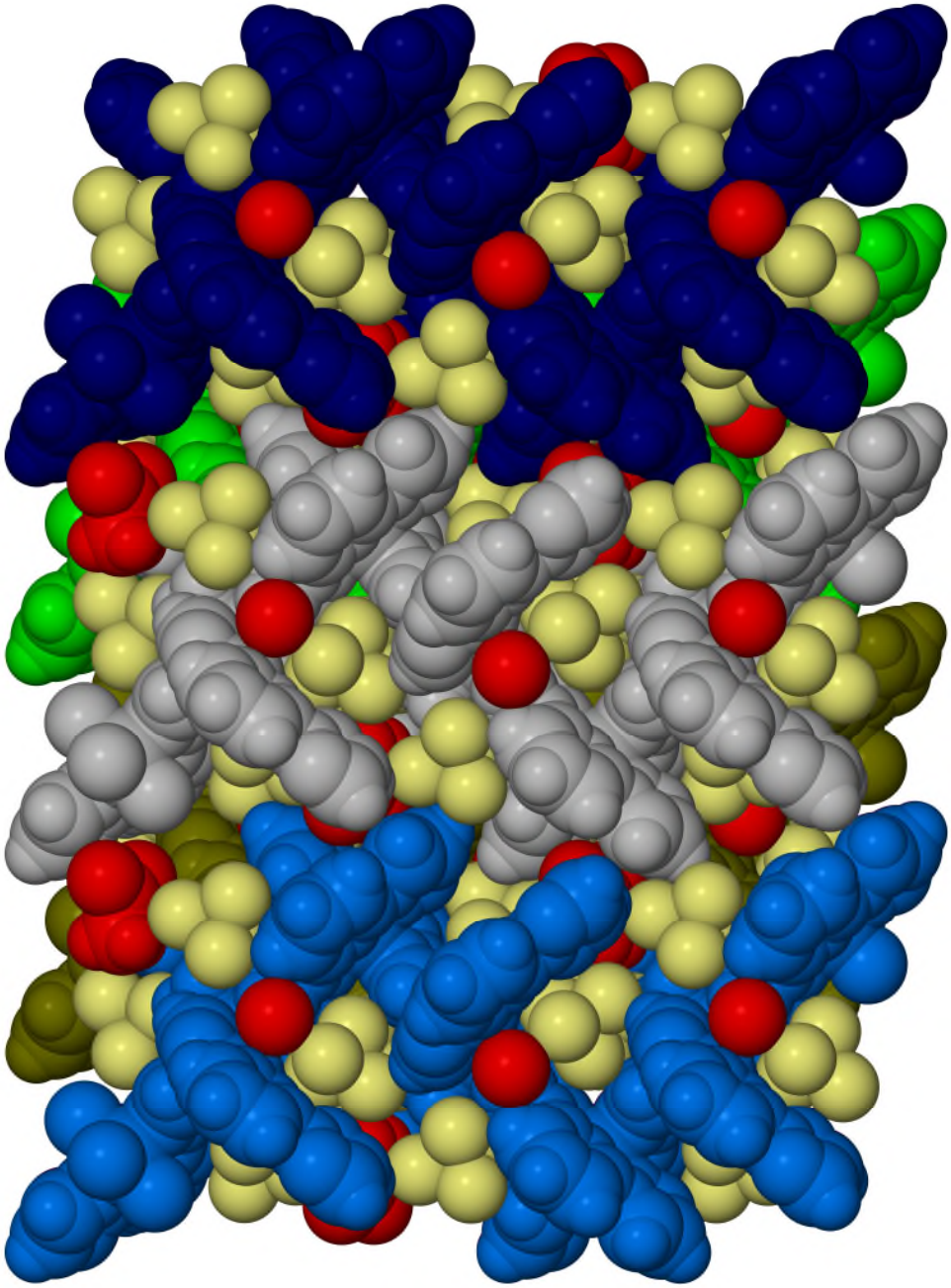

Figure S12 Space filling plot of the packing diagram in Figure S11. Only one orientation of the disordered residues is shown in this view, but the colour scheme is the same as in Figures S10 and S11.

The isolated red spheres are the partial lattice water site.

Despite the appearance given by Figure S11, there is no porosity in this structure.

References

1 L. Wang, N. Liu and B. Dai, *RSC Adv.*, 2015, **5**, 82097.

2 L. J. Kershaw Cook and M. L. A. Ramsay, *Inorg. Chem. Commun.*, 2019, **104**, 207.

3 G. M. Sheldrick, *Acta Cryst. Sect. C.: Struct. Chem.*, 2015, **71**, 3.

4 L. J. Barbour, *J. Supramol. Chem.*, 2001, **1**, 189.

5 O. V. Dolomanov, L. J. Bourhis, R. J. Gildea, J. A. K. Howard and H. Puschmann, *J. Appl. Cryst.*, 2009, **42**, 339.

6 C. J. O'Connor, *Prog. Inorg. Chem.*, 1982, **29**, 203.

7 A. Santoro, L. J. Kershaw Cook, R. Kulmaczewski, S. A. Barrett, O. Cespedes and M. A. Halcrow, *Inorg. Chem.*, 2015, **54**, 682.

8 P. Guionneau, M. Marchivie, G. Bravic, J.-F. Létard and D. Chasseau, *Top. Curr. Chem.*, 2004, **234**, 97.

9 J. K. McCusker, A. L. Rheingold and D. N. Hendrickson, *Inorg. Chem.*, 1996, **35**, 2100.

10 I. Capel Berdiell, R. Kulmaczewski and M. A. Halcrow, *Inorg. Chem.*, 2017, **56**, 8817.

11 M. A. Halcrow, *Chem. Soc. Rev.*, 2011, **40**, 4119.